

Article

Genome-Wide Identification and Characterization of the Superoxide Dismutase (SOD) Gene Family in Pakchoi and the Role of the *BchFSD2* Gene in the Salt Stress Toleran

Yuqi Zhou, Shuhao Li, Shengxiang Ran, Yang Xu, Maomao Hou, Mingxuan Han and Fenglin Zhong *

College of Horticulture, Fujian Agriculture and Forestry University, Fuzhou 350002, China; zhouyuqi@fafu.edu.cn (Y.Z.); being@fafu.edu.cn (S.L.); sxran0601@fafu.edu.cn (S.R.); 2210306001@fafu.edu.cn (Y.X.); houmaomao@fafu.edu.cn (M.H.); hanmx99@fafu.edu.cn (M.H.)
* Correspondence: zhong591@fafu.edu.cn

Abstract: Superoxide dismutase (SOD) is an important antioxidant metalloenzyme present in plants that plays a vital role in plant growth and development, but studies on the SOD gene family in Pakchoi are lacking. In this study, we identified 13 SOD genes from pakchoi, including three *MnSODs*, five *Cu/ZnSODs*, and five *FeSODs*. Through structural analysis, the gene structures and motif patterns in the three subfamilies showed a high degree of conservation. From an evolutionary point of view, gene duplication is an important pathway driving the evolutionary development of the SOD gene family. In addition, by analyzing the structure and function of *BchSOD* proteins, most of the genes were shown to be involved in different developmental stages of pakchoi, and their expression was shown to be regulated by external conditions such as light, phytohormones, and abiotic stress. qPCR results revealed that *BchSODs* were expressed in different parts of pakchoi, and most of the genes were expressed in response to abiotic stresses (salt and drought) and hormones (GA and MeJA). In addition, the *BchFSD2* gene was studied in depth, and subcellular localization confirmed that the *BchFSD2* gene was expressed in plant chloroplasts. Overexpression of *BchFSD2* promoted salt tolerance, limited superoxide anion and MDA production, and increased antioxidant enzyme activities in Arabidopsis. In summary, the *BchSOD* gene family was comprehensively analyzed in this study to provide new insights for a better understanding of *BchSOD* function and to improve salt tolerance in pakchoi.

Keywords: pakchoi; superoxide dismutase (SOD); genome-wide characterization; abiotic stress



Citation: Zhou, Y.; Li, S.; Ran, S.; Xu, Y.; Hou, M.; Han, M.; Zhong, F. Genome-Wide Identification and Characterization of the Superoxide Dismutase (SOD) Gene Family in Pakchoi and the Role of the *BchFSD2* Gene in the Salt Stress Toleran.

Agronomy **2024**, *14*, 384. <https://doi.org/10.3390/agronomy14020384>

Academic Editor: Urmila Basu

Received: 26 January 2024

Revised: 13 February 2024

Accepted: 13 February 2024

Published: 16 February 2024



Copyright: © 2024 by the authors. Licensee MDPI, Basel, Switzerland. This article is an open access article distributed under the terms and conditions of the Creative Commons Attribution (CC BY) license (<https://creativecommons.org/licenses/by/4.0/>).

1. Introduction

Plants live in ever-changing environments that typically have periods of unfavorable or stressful conditions that affect plant growth and development. These negative environmental situations involve biotic stresses, such as predator attacks, as well as abiotic stresses, such as heat, nutrient deficiencies, drought, cold, and an overabundance of salts [1]. Plant life processes are bound to involve reactive oxygen species (ROS) production. ROS consist of oxygen radicals such as superoxide ($O_2^{\cdot -}$), hydroxyl (OH), and other nonradial species such as hydrogen peroxide (H_2O_2) [2]. However, various biotic and abiotic stressors can influence ROS homeostasis. In addition, many detrimental effects can result in excessive accumulation of ROS, causing oxidative stress, which can lead to damage to essential cellular components, including nucleic acids, proteins, carbohydrates, and lipids, and may ultimately cause programmed cell death [3,4].

In an attempt to defend themselves against excess ROS due to deleterious effects, plant cells and their organelles employ antioxidant mechanisms. Cellular antioxidant mechanisms are among the major ways to defend against various types of stresses [4]. The plant antioxidant defense system includes numerous nonenzymatic and enzymatic antioxidants. The principal nonenzymatic antioxidants consist of ascorbic acid (ASA),

glutathione (GSH), and phenolic compounds. On the other hand, enzymatic antioxidants include superoxide dismutase (SOD), catalase (CAT), ascorbate peroxidase (APX), and glutathione reductase (GR) [5]. Among the many known antioxidant enzymes, SOD is commonly found in all aerobic organisms and in all subcellular cells susceptible to ROS-mediated oxidative stress, and it is one of the most potent components of the antioxidant defense against ROS toxicity in plant cells. It has been shown that $O_2^{\cdot-}$ is eliminated by SOD-catalyzed disproportionation, where one $O_2^{\cdot-}$ is converted into H_2O_2 and the other into O_2 [4]. According to the metal cofactors, plant SODs include four main types: *FeSODs* (iron cofactors), *MnSODs* (manganese cofactors), *Cu/ZnSODs* (with Cu and Zn serving as cofactors, where Cu is the redox-active catalytic metal), and *NiSODs* (nickel cofactors). To date, no NiSOD has been identified in plants [6].

In recent years a large number of researchers have shown that the SOD gene plays a crucial position in plant resistance to harsh environmental conditions and is responsive to a vast array of environmental signals. For instance, several studies have identified SODs as pivotal genes that mediate immunity to heavy metal toxicity in tobacco [7]. Shiraya [8] et al. identified MSD1 as a unique Golgi somatic type of SOD in heat-tolerant rice varieties (*Oryza sativa*) that enhances the ability of plants to adapt to heat. In addition, Mosa [9] et al. reported that the expression of the *Cu-ZnSOD* gene was induced in cucumber plants (*Cucumis sativus*) by copper nanoparticles. Taken together, the results of these studies indicate that plant stress tolerance can be enhanced by increasing SOD activity and the expression of SOD-encoding genes. To date, genome-wide identification and studies of the SOD gene family have been carried out in a number of plants, including *Nicotiana tabacum* [7], rapeseed [10], tomato [11], *Larix kaempferi* [12], *Salvia miltiorrhiza* [13], and grapevine [14].

Pakchoi (*Brassica campestris* L. ssp. *Chinensis*) is a leafy vegetable widely grown in Asian countries. To date, genome-wide characterization of the SOD gene family in pakchoi has not been reported. In this study, we identified the SOD gene family in pakchoi at the genome-wide level and systematically analyzed its physicochemical properties, gene structure, homology, and phylogenetic developmental relationships. The cis-acting elements of the promoter region of the *BchSOD* genes were also predicted and analyzed. In addition, the *BchSOD* genes were analyzed for tissue-specific expression as well as for expression patterns in response to abiotic stresses (salt and drought) and hormone treatments (gibberellin and methyl jasmonate). We also performed subcellular localization and constructed an overexpression vector of the abiotic stress-sensitive gene *BchFSD2* to investigate further its function and regulatory network under salt stress. This study lays the foundation for further research on the function of the SOD gene in pakchoi under different external influences.

2. Materials and Methods

2.1. Genome-Wide Identification of SOD in Pakchoi

In this study, we used BLASTP and the Hidden Markov Model to identify SOD genes in pakchoi. The whole pakchoi genomic dataset, which included coding sequence (CDS), genetic feature format (GFF), and protein sequence information, was previously evaluated by our laboratory and downloaded from the figshare database (<https://figshare.com/articles/dataset/Thegenomeannotationinformationofpakchoi/19589524> (accessed on 1 March 2023)). The protein sequences of the SODs described in the model plant *Arabidopsis* were downloaded from the NCBI database (<https://www.ncbi.nlm.nih.gov/gene/> (accessed on 1 July 2023)). Using the *Arabidopsis* SOD protein sequence as the query sequence, the BLAST Zone program of Tbttools was used to search for the pakchoi SOD protein. Furthermore, all the predicted pakchoi SOD family members were confirmed through Pfam (<http://pfam.xfam.org/> (accessed on 1 July 2023)) [15]. The physicochemical parameters, including length, molecular weight, isoelectric point, GRAVY, and instability index, were analyzed by the online tool ExPASy server (<https://web.expasy.org/> (accessed on 1 March 2023)) [16]. Tbttools was used to map the SOD genes to the pakchoi chromo-

somes [17], and the subcellular location of each protein was investigated by WoLF PSORT (<https://wolfpsort.hgc.jp/> (accessed on 1 July 2023)).

2.2. Phylogenetic Analysis of BchSOD Genes

The SOD amino acid sequences of different plant species, such as *Brassica rapa* and *Brassica oleracea*, were downloaded from the JGI Phytozome 12.0 database (<https://phytozome-next.jgi.doe.gov/> (accessed on 2 July 2023)) [10]. For further classification, we constructed a phylogenetic tree of the *B. rapa*, *B. oleracea*, *B. chinensis*, and *A. thaliana* protein sequences. The sequences were aligned using MEGA7.0 software, and a phylogenetic tree was constructed using the neighbor-joining (NJ), maximal and minimal method with a 1000 bootstrap and other parameters set to default values [18]. Then, the Evolview v3 website (<https://www.evolgenius.info/evolview/>, (accessed on 2 July 2023)) [19] was used to visualize the phylogenetic tree.

2.3. Analysis of BchSOD Gene Structures, Conserved Motifs, and Conserved Domains

The *BchSOD* gene structures were analyzed using Tbttools V2.042 software. The MEME tool (<https://meme-suite.org/meme/tools/meme>, (accessed on 3 July 2023)) was used to predict the conserved motifs, with the motif value set to ten, and the site distribution set for any number of repetitions and other parameters at default. Then, Tbttools V2.042 software was used to visualize the conserved motifs.

2.4. Chromosomal Localization and Synteny Analysis of BchSOD Genes

The chromosomal distribution and collinearity mapping of the *BchSOD* genes were performed using the advanced circos module in Tbttools [17]. Then, synteny analysis of the SOD genes was performed with the One Step MCScanX module of Tbttools from *B. rapa*, *B. oleracea*, *B. chinensis*, and *A. thaliana*.

2.5. Cis-Acting Regulatory Elements in Promoter Analysis of BchSOD Genes

The promoter sequences of the Pakchoi *BchSOD* genes (2000 bp upstream) were obtained by the Gtf/Gff3 Sequence Extraction module of Tbttools. The online tool PlantCARE (<http://bioinformatics.psb.ugent.be/webtools/plantcare/html/> (accessed on 5 July 2023)) was used to analyze the cis-acting regulatory elements.

2.6. Prediction of the 2D and 3D Structure of BchSOD Proteins

The secondary structure of the *BchSOD* proteins was predicted using the Prabi website (Available online: https://npsa-prabi.ibcp.fr/cgi-bin/npsa_automat.pl?page=/NPSA/npsa_sopma.html (accessed on 12 July 2023)). The predicted tertiary structures of *BchSOD* proteins were visualized through the SWISS-MODEL website (Available online: <https://www.swissmodel.expasy.org/> (accessed on 12 July 2023)) with default parameters [20].

2.7. Plant Materials and Growth Conditions

In this study, the hybrid pakchoi variety 'Jinpin Hanchun' (Jinpin Agriculture, Fujian, China) was used as a test material, and experimental treatments were carried out. After the seeds were soaked and germinated, the uniformly growing plants were selected for hydroponics with Hoagland nutrient solution and cultured under a photoperiod of 12 h of light with a light intensity of approximately $180 \pm 15 \mu\text{mol}\cdot\text{m}^{-2}\cdot\text{s}^{-1}$ PPFD at a temperature of 25 ± 3 °C. The plants were treated when four leaves and one heart were present. To simulate salt and drought conditions, 150 Mm NaCl [10] and 10% PEG6000, respectively, were added to the culture solution. Tender leaves were collected from treated plants in three independent biological replicates at 0 h, 12 h, 24 h, 36 h, and 48 h after each treatment. For phytohormone treatments, leaves were sprayed once with freshly prepared working solutions of 100 μM GA [10] or 100 μM MeJA. Tender leaves were collected from treated plants in three independent biological replicates at 0 h, 2 h, 4 h, 6 h, and 8 h after each

treatment. Finally, all the samples were packed in aluminum foil, immediately submerged in liquid nitrogen, and stored at -80°C until further analysis.

2.8. *BchSOD* Gene Expression Pattern Analysis in Different Tissues

To analyze the specific expression of the *BchSOD* genes in different tissues, five leaves and one heart, roots, petioles, cotyledons, and true leaves of 'Jinpin Hanchun' pakchoi plants hydroponically cultivated in Hoagland nutrient solution were selected as experimental materials. The samples were frozen in liquid nitrogen and then stored at -80°C .

2.9. RNA Extraction and qRT-PCR Analyses

Total RNA extraction and cDNA synthesis were performed using a FastPure Plant Total RNA Isolation Kit (Vazyme Biotech, Nanjing, China) and FastKing gDNA Dispelling RT SuperMix (TranGen Biotech, Beijing, China) according to the manufacturer's instructions. qRT-PCR was performed on a Roche LightCycler 96 PCR system, following the recommended guidelines for $2\times$ RealStar Green Fast Mixture (GenStar Biotech, Beijing, China). The primers for qPCR were designed using Primer Premier 5.0 and are listed in Supplementary Table S1. The actin gene of pakchoi was used as an internal control. Three biological replicates were carried out for each cDNA sample. The cycle threshold (CT) data that were obtained were calculated using the $2^{-\Delta\Delta\text{CT}}$ method to determine the relative expression of the *BchSOD* genes [21]. Finally, heatmaps were created using Tbtools V2.042 software.

2.10. Subcellular Localization of *BchFSD2*

To further determine the subcellular localization of the *BchFSD2* gene, the protein-coding region of the target gene was amplified using Phanta Max Super-Fidelity DNA Polymerase (Vazyme Biotech, Nanjing, China). The primers for PCR were designed using Primer Premier 5.0 and are listed in Supplementary Table S2. The CDS of *BchFSD2* was cloned and inserted into the PGWB605 vector by the Gateway method using a gateway kit (Thermo Fisher Scientific, Shanghai, China) to generate the C-terminal fusion green fluorescent protein (GFP) construct 35: *BchFSD2*-GFP. This construct was subsequently transformed into *Agrobacterium tumefaciens* receptor GV3101 cells (HeRui, Fujian, China). The injection method was used for transient expression in tobacco leaves, after which the plants were subjected to darkness for 24 h and subsequently incubated under normal conditions for 48 h. Then, fluorescence was observed under a confocal microscope (Olympus Fv1200, Shanghai, China).

2.11. Transformation of *Arabidopsis thaliana* Overexpressing the *BchFSD2* Gene

The recombinant *Agrobacterium tumefaciens* plasmid harboring the target gene *BchFSD2* was transformed into wild-type *Arabidopsis thaliana* using the floral dip method [22]. After the T0 generation was harvested, the plants were sterilized and sown in 1/2 MS medium supplemented with 10 mg/L glufosinate-ammonium antibiotic, and when four true leaves were growing and normal-growing *Arabidopsis* plants were regarded as positive seedlings, they were transplanted into nutrient soil and considered the T1 generation, and the plants were subjected to PCR. Subsequently, the procedure was repeated until the pure strain of the T3 generation was obtained. Finally, the overexpression efficiency of the T3 pure strain *BchFSD2* was verified by qRT-PCR.

2.12. Abiotic Stress Treatment and Related Physiological Index Detection

Transgenic *Arabidopsis thaliana* (L1) and wild-type *Arabidopsis* (WT) plants were cultured in 1/2 MS medium until four leaves were reached (12 days) and subsequently transferred to soil for 11 days for salt stress and drought stress treatments. For the salt stress treatments, L1 and WT plants were watered with 150 Mm NaCl at 3 d intervals, while the transgenic *Arabidopsis* control (L1-CK) and wild-type control (WT-CK) plants were wa-

tered at the same time. Samples were taken after 9 days of salt treatment for physiological data determination.

Physiological indices were mainly determined for hydrogen peroxide (H₂O₂), superoxide anion, and malondialdehyde (MDA) contents as well as superoxide dismutase (SOD), peroxidase (POD) and catalase (CAT) activity assays in experimental (L1 and WT) and control (L1-CK and WT-CK) cabbages under salt stress. The H₂O₂ content was determined using the H₂O₂ assay kit (Keming, Suzhou, China). About 0.15 g of leaves were ground and lysed in 1 mL of lysing solution, followed by the addition of reaction solution according to the instructions of the kit for the reaction. The absorbance was measured at 415 nm, and then the standard curve was used in order to calculate the content of H₂O₂. Superoxide anion and MDA contents, as well as SOD, POD, and CAT activities, were also determined using the corresponding assay kits (Keming, Suzhou, China), respectively. Tissue extraction was performed as previously described, with specific experiments also following the instructions provided with the kits, and three technical replicates were performed for each treatment.

3. Results

3.1. Identification and Characterization of the SOD Gene Family in Pakchoi

Based on the results of the HMM search and BLASTP, 13 *BchSOD* genes were found in pakchoi. According to structural domain analysis, the numbers of proteins with a *Mn-SOD* domain (Pfam:02777), a *Cu/Zn-SOD* domain (Pfam: 00080), and a *Fe-SOD* domain (Pfam:00081) were 3, 5, and 5, respectively. Therefore, based on their species name and Pfam types, these genes were named *BchMSD1*–*BchMSD3*, *BchCSD1*–*BchCSD5*, and *BchFSD1*–*BchFSD5*, respectively (Table 1). The physical and chemical characteristics of the 13 *BchSODs* are shown in Table 1. All 13 *BchSOD* genes were located in the A subgenome. The protein and CDS lengths and molecular weights were 152–299 amino acids, 459–900 bp, and 37.83–73.4 kDa, respectively. Moreover, the instability exponents of the *BchSOD* proteins varied from 41.68 to 66.86; the isoelectric point varied from 5.08 to 5.21, indicating that all the members of *BchSOD* are acidic; and the GRAVY values ranged from 0.684 to 1.017, indicating that all the *BchSODs* are hydrophobic proteins. The subcellular localization results revealed that six proteins (*BchCSD3*, *BchCSD4*, *BchFSD1*, *BchFSD3*, *BchFSD4*, and *BchFSD5*) were predicted to localize to the chloroplast, three proteins (*BchMSD2*, *BchMSD3*, and *BchFSD2*) were located on the mitochondria, three proteins (*BchCSD1*, *BchCSD2*, and *BchCSD5*) were located in the cytoplasm, and the remaining protein (*BchMSD1*) was located in the extracellular region space (Table 1).

Table 1. The characteristics of 13 SOD genes in pakchoi.

Gene Name	Gene ID	Genomic Position (bp)	Protein Length (aa)	CDS Length (bp)	Molecular Weight/(Da)	Isoelectric Point (PI)	GRAVY	Instability Index	Subcellular Localizations
BchMSD1	Bch09G054140.1	A09-53671833:53673122(–)	241	726	60.26	5.11	0.851	55.34	Extracellular
BchMSD2	Bch01G046450.1	A01-34214509:34215993(–)	231	696	56.59	5.14	0.766	41.68	Mitochondrial
BchMSD3	Bch05G042360.1	A05-35515870:35517513(–)	231	696	56.76	5.15	0.736	44.12	Mitochondrial
BchCSD1	Bch06G006380.1	A06-3784500:3786799(+)	153	459	37.83	5.21	0.734	57.62	Cytoplasm
BchCSD2	Bch09G070780.1	A09-61463615:61465502(–)	152	459	37.95	5.21	0.704	53.29	Cytoplasm
BchCSD3	Bch07G020850.1	A07-18191165:18192695(+)	162	489	42.12	5.14	1.017	66.86	Chloroplast
BchCSD4	Bch04G023970.1	A04-18398587:18400291(+)	207	624	52.88	5.11	0.864	58.93	Chloroplast
BchCSD5	Bch10G024890.1	A10-20006809:20008560(–)	162	489	40.15	5.21	0.762	57.07	Cytoplasm
BchFSD1	Bch03G016650.1	A03-7871955:7873744(+)	299	900	73.4	5.1	0.802	47.6	Chloroplast
BchFSD2	Bch01G016870.1	A01-8554165:8556874(+)	264	795	66.65	5.08	0.897	61.46	Mitochondrial
BchFSD3	Bch06G036350.1	A06-38063266:38064684(+)	263	792	65.08	5.14	0.713	49.96	Chloroplast
BchFSD4	Bch09G007260.1	A09-3927405:3929188(–)	263	792	65.2	5.14	0.708	51.3	Chloroplast
BchFSD5	Bch09G007220.1	A09-3910081:3911975(–)	269	810	66.76	5.14	0.687	49.65	Chloroplast

3.2. Phylogenetic Analysis of SOD Genes

We constructed a phylogenetic tree by comparing the full-length sequences of SOD proteins from *A. thaliana*, *B. oleracea*, *B. napus*, and *B. chinensis* to determine the evolutionary relationship of SOD in different species. The 66 SODs were categorized into three classes according to their structural domain and phylogenetic tree (Figure 1 and Figures S2 and S3). The results indicated that the *Cu/Zn-SOD* group included twenty-eight SOD members (six

BolSODs, fourteen *BnSODs*, five *BchSODs*, and three *AtSODs*), the *Mn-SOD* group included fourteen *SOD* members (three *BolSODs*, six *BnSODs*, three *BchSODs*, and two *AtSODs*), and the *Fe-SOD* group included twenty-four *SOD* members (five *BolSODs*, eleven *BnSODs*, five *BchSODs*, and three *AtSODs*). Moreover, *BchCSD5* and *BnCSD7*, *BchCSD2* and *BnCSD6*, *BchCSD1* and *BolCSD2*, *BchMSD2* and *BnMSD1*, *BchMSD3* and *BolMSD1*, *BchMSD1* and *BnMSD3*, *BchFSD1* and *BnFSD2*, *BchFSD2* and *BolFSD4*, *BchFSD5* and *BnFSD4*, *BchFSD4* and *BolFSD3* were the smallest branches, respectively; furthermore, the *BchSODs* were closer to the *BolSODs* and *BnSODs* during the evolutionary process.

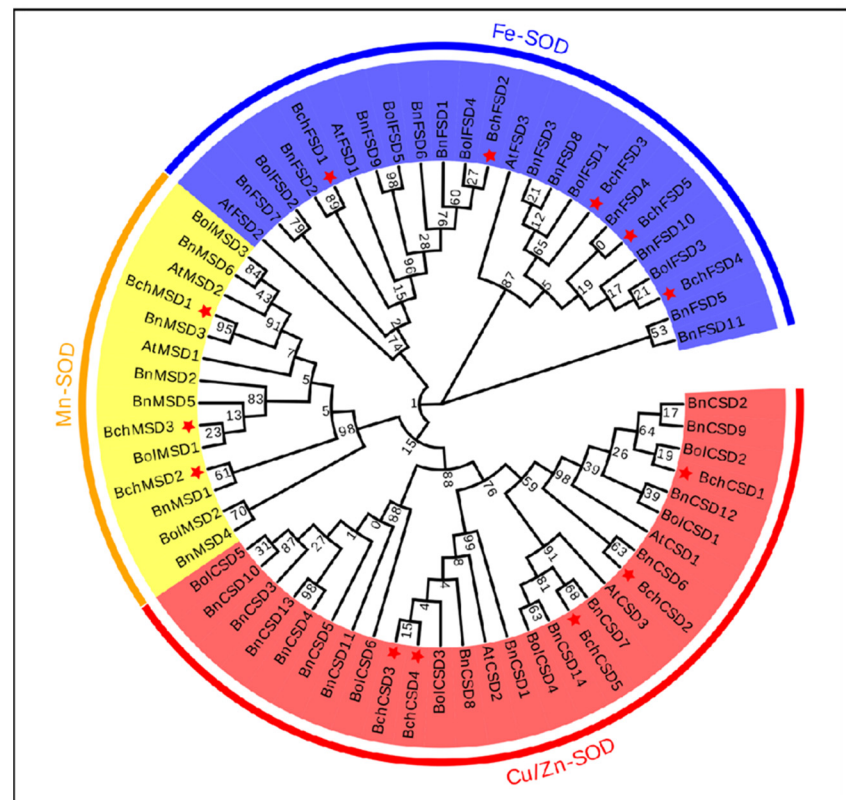


Figure 1. Phylogenetic tree of *SOD* proteins from *A. thaliana*, *B. oleracea*, *B. napus*, and *B. chinensis* (the neighbor-joining (NJ) method). Different colors represent different branches: *Fe-SOD* (blue), *Cu/Zn-SOD* (red), and *Mn-SOD* (yellow). Moreover, *BchSOD* is labeled with a red star. At: *Arabidopsis thaliana*, Bol: *Brassica oleracea*, Bn: *Brassica napus*, Bch: *Brassica chinensis*.

3.3. Conserved Motifs and Gene Structures Analysis of *BchSOD* Genes

To understand the structural variation of the *BchSOD* proteins and determine their functions, we analyzed the conserved motifs of the *BchSOD* genes using the MEME tool and visualized them with TBtools (Figure 2B and Table S3). The results revealed that 10 motifs were present in *BchSODs* (Figure 2D). The conserved motifs of the *BchSOD* proteins varied from two to seven, and the analysis revealed that similar related members in the same subfamily had the same motif formation. Motifs 1, 4, and 3 were predicted in all the *Fe-SOD* and *Mn-SOD* members. Motif 5 was predicted for most proteins of the *Fe-SOD* and *Cu/Zn-SOD* genes, except for *BchCSD3*, *BchFSD1*, and *BchFSD2*. Interestingly, motifs 2 and 10 existed only in *Cu/Zn-SOD* subfamily members, motif 9 was a unique conserved motif in *Mn-SOD* subfamily members, and motifs 6 and 8 existed only in *Fe-SOD* subfamily members. Further examination of the motif logos plot (Figure 2D) revealed that motifs 6, 7, and 9 were more conserved. Therefore, according to our predictions, the members of the *Fe-SOD* and *Mn-SOD* subgroups were more conserved.

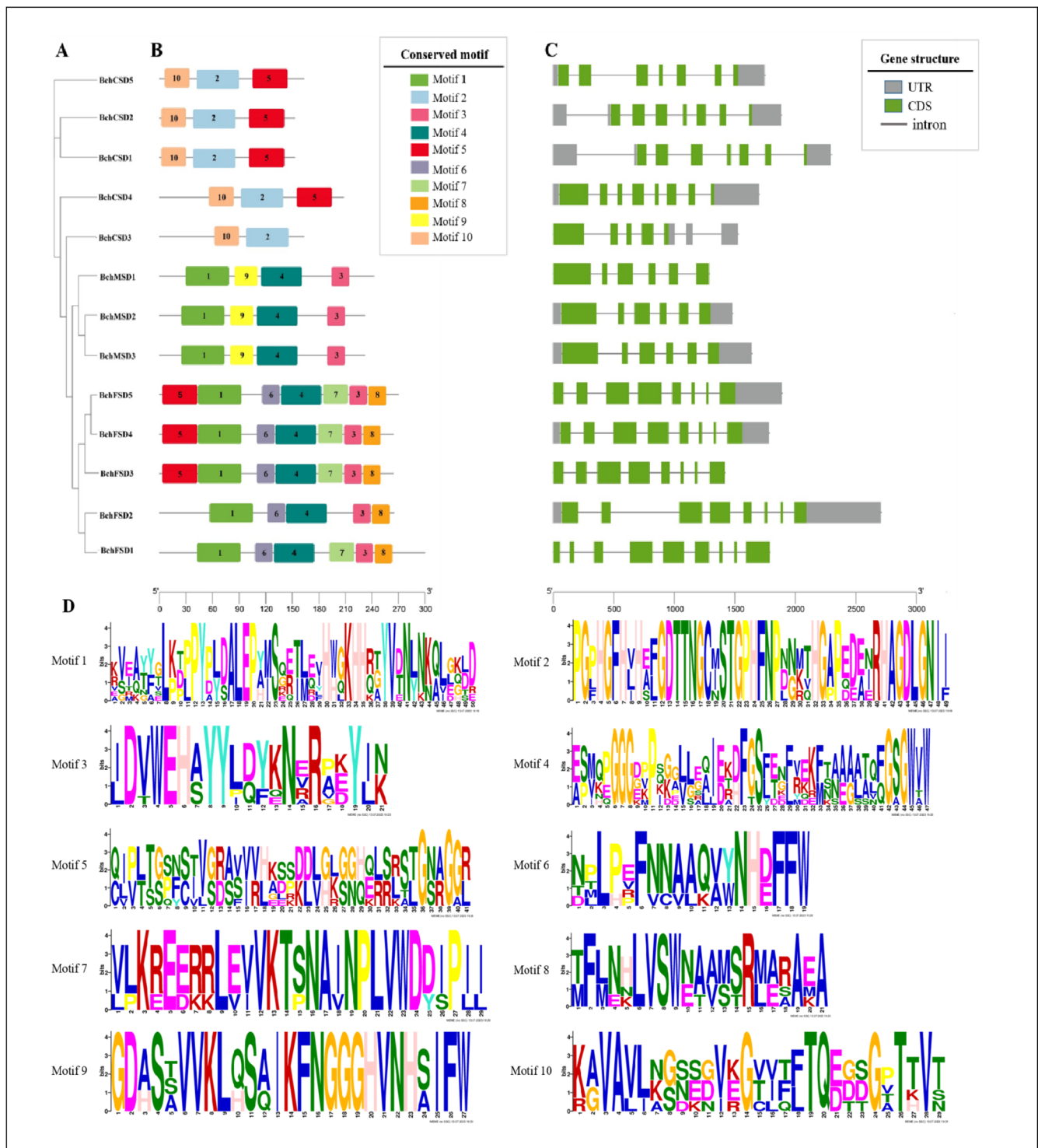


Figure 2. Phylogenetic tree, conserved motifs, gene structures, and motif logos of *BchSODs*. (A) Phylogenetic tree of *BchSODs*. (B) Conserved motifs of *BchSODs*. Ten motifs in *BchSOD* were detected using the MEME tool and were labeled with different colors. (C) Gene structure of *BchSODs*. The gray lines represent introns, and the green and gray boxes represent CDSs and UTRs, respectively. (D) Logos of ten detected motifs of *BchSODs*.

The study of gene structure has aided in understanding the evolution of the *SOD* family of genes in pakchoi. The results demonstrated that the quantities of exons and introns in the *BchSOD* genes were 5–9 and 5–8, respectively (Figure 2C). The *Mn-SOD*

subfamily includes six exons and five introns. The *Cu/Zn-SOD* group had 6 to 7 exons and 5 to 8 introns. The *Fe-SOD* group contained eight exons and seven introns, except for *BchFSD1*, which contained nine exons and eight introns. Notably, the *BchMSD2* and *BchMSD3* genes exhibited similar gene structures. In summary, the *BchSOD* genes differed significantly in terms of the number of exons and introns but exhibited similar intron/exon patterns within the same evolutionary branch.

3.4. Analysis of Cis-Acting Elements in Promoters of *BchSOD* Genes

SOD genes play a crucial role in the response to external stresses. We analyzed cis-acting elements in the promoters of *BchSOD* genes by using 2000 bp upstream regions to investigate hypothetical cis-acting elements that play critical roles in stress, light, and hormone modulation. Overall, 314 cis-acting elements were identified in the *BchSOD* genes (Figure 3), and additional detailed information on the cis-acting elements is displayed in Table S4.

Cis-acting elements involved in defense and stress responsiveness, such as drought-responsive elements (MBSs), anaerobic-responsive elements (AREs), low temperature-responsive elements (LTRs), and stress-responsive elements (TC-rich repeats), were detected in the promoters of the *BchSOD* genes. Furthermore, the drought-responsive element MBS was found primarily in the promoters of the *BchMSD* group and *BchFSD* genes. Moreover, many phytohormone-related cis-acting elements, which included abscisic-acid responsiveness (ABRE), MeJA-responsiveness (TGACG motif and CGTCA motif), auxin responsiveness (TGA element), gibberellin responsiveness (GARE motif and P-box) and salicylic-acid responsiveness (TCA element), were identified in the promoter region of the *BchSOD* genes. Most of the *BchSOD* genes were identified by analysis as having the MeJA-responsive TGACG motif (except for *BchCSD1* and *BchCSD4*) and the CGTCA motif (except for *BchCSD1*, *BchCSD4*, and *BchFSD5*). Elements related to the auxin response are dispersed only within the promoters of MSD and CSD subfamily genes. Elements related to abscisic acid, gibberellin, and salicylic-acid responses are widely distributed among most *BchSOD* genes. These findings suggest that auxin plays a supervisory role in the MSD and CSD subfamilies and that phytohormones may have a regulatory effect on the control of *BchSOD* gene expression. Moreover, seven light-responsive genes (G-box, GT1-motif, Box 4, I-box, AE-box, chs-CAM1a, and TCT-motif) were found in the *BchSOD* gene promoter, among which I-box, AE-box, chs-CAM1a, and TCT-motif elements were distributed only in the *BchCSD* subfamily and *BchFSD* subfamily genes. Overall, the study showed that *BchSOD* genes are involved in the regulation of gene expression at different developmental stages and in the response to light, phytohormones, and abiotic stress in pakchoi.

3.5. Chromosomal Locations and Synteny Analysis of *BchSOD* Genes

To understand the tandem and segmental relationships of *SOD* genes in pakchoi, we further analyzed the chromosomal locations of *BchSODs*. Therefore, the chromosomal locations of 13 *BchSOD* gene pairs are shown in Figure 4. Eight out of the ten chromosomes harbored *BchSODs*. Detailed analysis revealed that chromosomes A03, A04, A05, A07, and A10 each contained one gene, chromosomes A01 and A09 each contained two genes, and chromosome A09 contained four genes. Moreover, one tandem repeat gene cluster in the *BchSOD* family was located on the A09 chromosome (*BchFSD4* and *BchFSD5*). With the exception of *BchMSD1* and *BchCSD5*, the remaining 11 genes had fragment duplication pairs (*BchMSD2/BchMSD3*, *BchCSD3/BchCSD4*, *BchCSD1/BchCSD2*, *BchFSD1/BchFSD2*, and *BchFSD3/BchFSD5*). This finding illustrates the importance of fragment duplication events in *BchSOD* diversity.

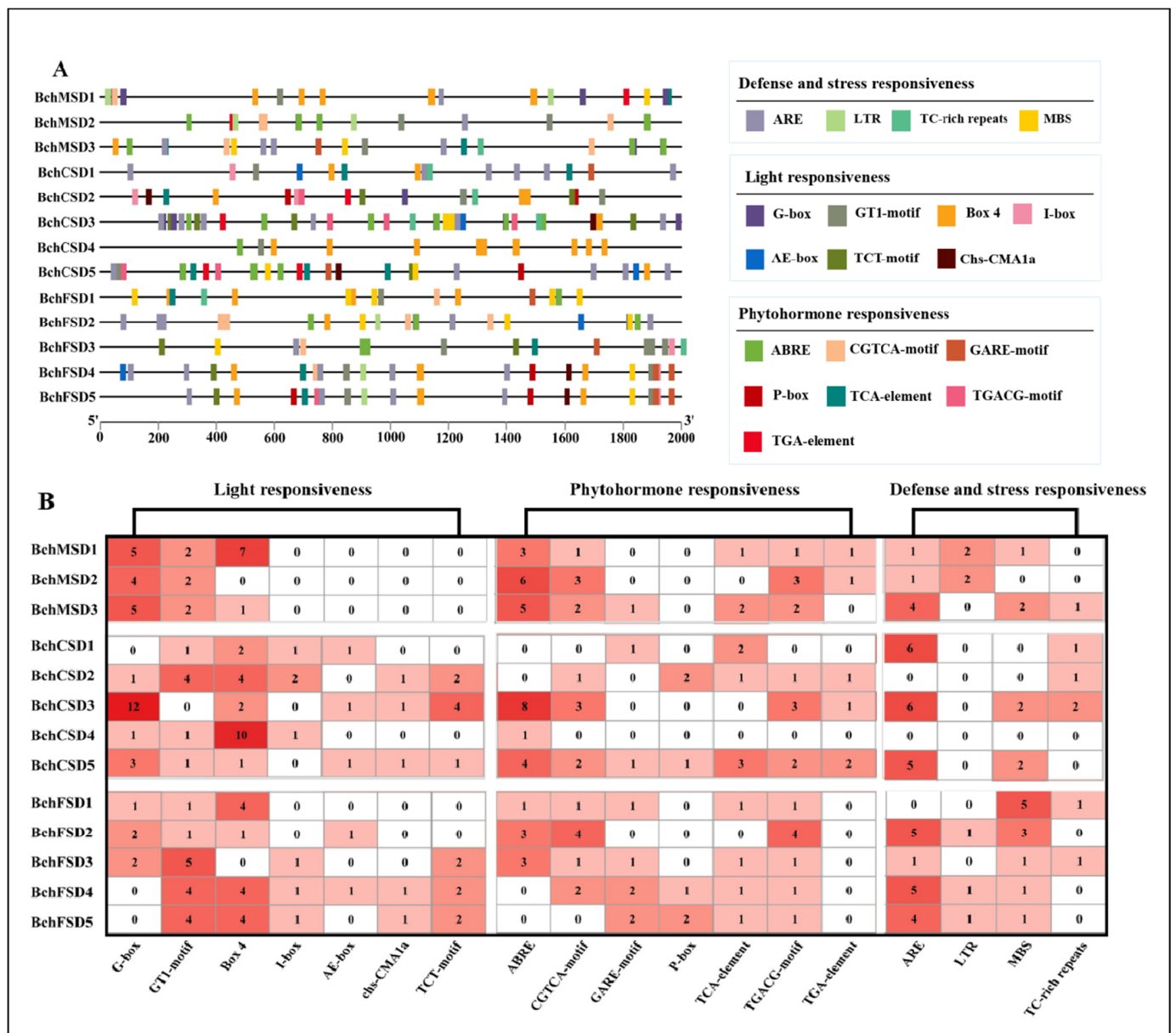


Figure 3. Cis-acting in the promoters of *BchSOD* genes. **(A)** Different color cubes display different cis-acting related to various defense and stress responsiveness, light responsiveness, and phytohormone responsiveness. **(B)** The frequencies of cis-acting elements are indicated by numbers and different colors.

A collinearity analysis revealed many orthologs of *SOD* genes among *B. chinensis* and two closely related species (*A. thaliana* and *B. oleracea*) (Figure 5). The analysis revealed that nine *B. chinensis* genes exhibited synteny with *AtSODs* and *BolSODs*. Moreover, the *BchSOD* gene family had 17 and 11 homologous gene pairs with those of the *BolSOD* and *AtSOD* genes, respectively. In conclusion, numerous *AtSOD* and *BolSOD* homologs exhibited syngeneic relationships with *BchSODs*, demonstrating that genome-wide duplications or segmentations play essential roles in the evolution of the *BchSOD* gene family.

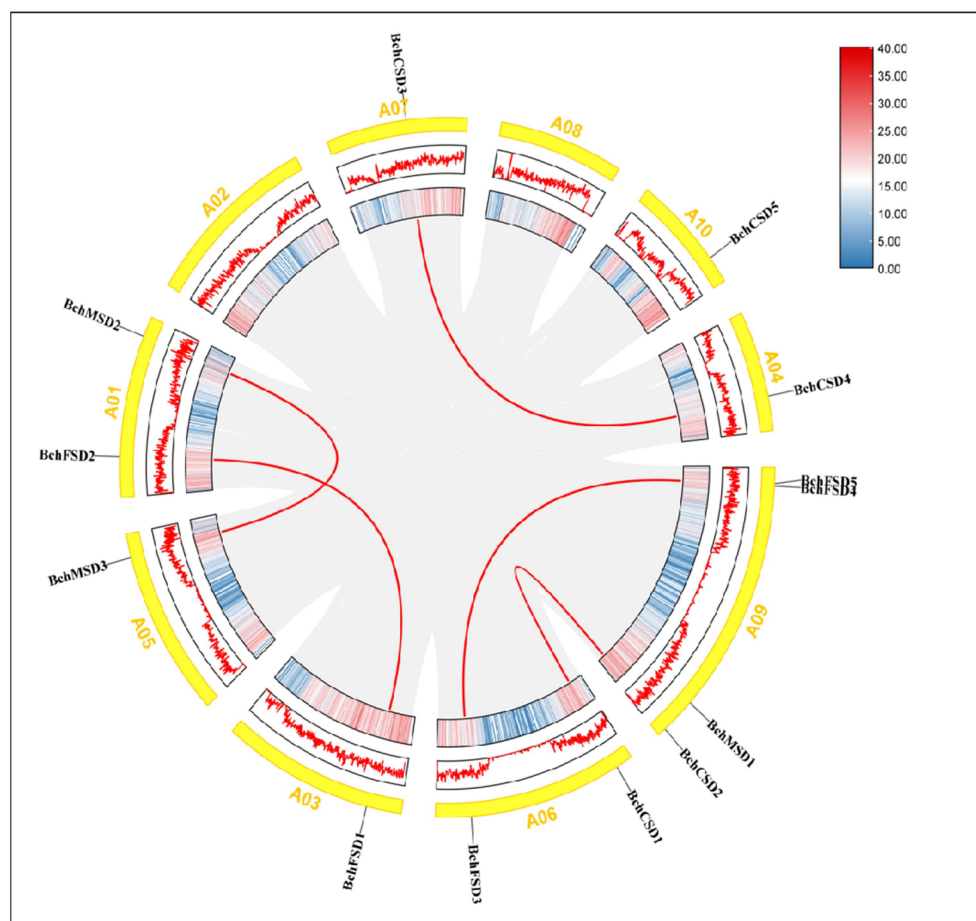


Figure 4. Chromosomal locations and interchromosomal associations of *BchSODs*. The Circos diagram is from the inside out, with the first and second layers being chromosome density and the third layer being the chromosomes. The gray background inside the circle represents all syntenic blocks in the *B. chinensis* genome, and the red lines represent homozygous *BchSOD* gene pairs.

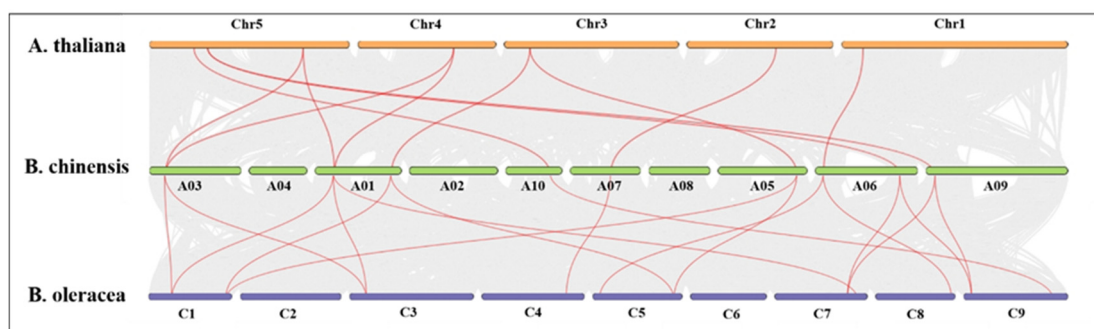


Figure 5. Collinearity analysis of *SOD* genes in *A. thaliana*, *B. chinensis*, and *B. oleracea* chromosomes. The grey areas in the figure indicate the collinear regions in *B. chinensis* and other plant genomes, and the red lines display the syntenic *SOD* gene pairs.

3.6. Analysis of the 2D and 3D Structures of *BchSOD*

Protein sequence structure can reflect protein function and lay the foundation for protein tertiary structure models. The 2D and 3D structures of the *BchSOD* proteins were analyzed (Figure S1 and Table S5), and the *BchSOD* protein structures were all composed of alpha helices, extended strands, beta turns, and random coils. Among these structures, those located in the same subfamily had similar structural models, while those in different

subfamilies exhibited significant differences in structure. The predicted *Mn-SOD* subfamily (*BchMSD1-BchMSD3*) protein models and *Fe-SOD* subfamily (*BchFSD1-BchFSD5*) protein models are mainly composed of alpha helices and contain a small amount of beta-turns. In contrast, the *Cu/Zn-SOD* (*BchCSD1-BchCSD5*) model is composed mainly of highly conserved beta-turns and contains some short alpha-helices.

3.7. Expression Patterns of *BchSOD* Genes in Different Tissues

The tissue-specific expression of the *BchSOD* genes was assessed at four different tissue sites (comprising the roots, petioles, cotyledons, and true leaves) of pakchoi by qRT-PCR. As illustrated in Figure 6 and Table S6, we have found that the CSD and MSD subgroups, except for *BchCSD5*, were expressed at low levels in petioles and cotyledons. Compared to those of other genes, the expression levels of *BchCSD3* and *BchCSD4* were lower in true leaves. Moreover, a high number of FSD subgroup genes were expressed in all four parts of the test, and the expression was greater in the true leaves than in the other parts. Additionally, *BchFSD1* was highly expressed in petioles, while other *BchSOD* genes exhibited decreased expression. This finding suggested that the FSD subgroup may have a vital effect on the growth of pakchoi.

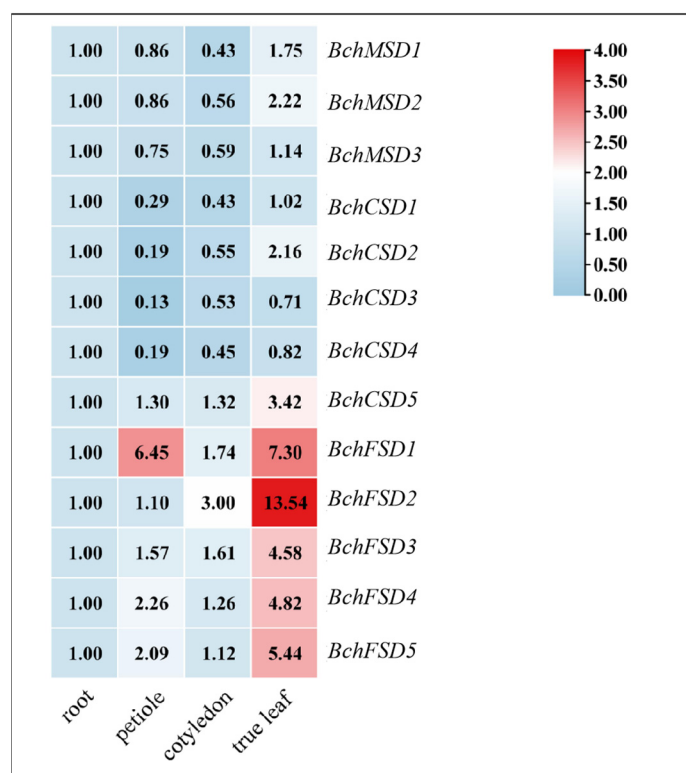


Figure 6. Relative expression levels of *BchSOD* genes in different pakchoi tissues. Red represents a high expression level, and blue represents a low expression level.

3.8. Expression of *BchSODs* in Response to Abiotic Stresses and Exogenous Phytohormones

To explore the expression levels of *BchSOD* genes in response to different phytohormone (MeJA and GA) and abiotic stress (salinity and drought) treatments, 13 *BchSOD* genes were analyzed via qRT-PCR to determine the transcriptional profiles (Figure 7 and Table S7). *BchSODs* exhibited diverse expression patterns under various stress conditions. Under salt stress, there was a significant upregulation of *BchCSD3* expression, which reached a maximum expression level at 12 h after NaCl treatment that was 3.97 times greater than that of the control. *BchCSD2* and *BchFSD2* were significantly upregulated at 48 h but not at other time points. Moreover, the expression of all the genes in the MSD subgroup did not change significantly. Under drought conditions, *BchCSD3*, *BchCSD4*, and *BchCSD5*

exhibited similar expression trends, with all exhibiting high expression at 12, 24, and 36 h. *BchFSD2* showed significant upregulation at 24 h but not at other time points. Moreover, *BchFSD4* and *BchFSD5* were significantly upregulated at 24 and 48 h, respectively. Under GA treatment, *BchFSD1* expression was markedly upregulated at all treatment time points, and it reached a maximum expression level at 8 h after NaCl treatment that was 2.13 times greater than that of the control. Moreover, the expression of four *BchSOD* genes, *BchCSD1*, *BchCSD2*, *BchCSD4*, and *BchFSD2*, was significantly upregulated at 2 and 8 h. *BchFSD4* and *BchFSD5* were significantly upregulated at 2 h, but not at other time points, resulting in significant variations. Under MeJA treatment, nearly all CSD subgroup and FSD subgroup member genes, except *BchCSD1*, *BchCSD2*, and *BchFSD1*, had relatively high expression levels. These results suggest that most *BchSOD* genes, especially those in the CSD and FSD subgroups, are involved in the phytohormone and abiotic stress response.

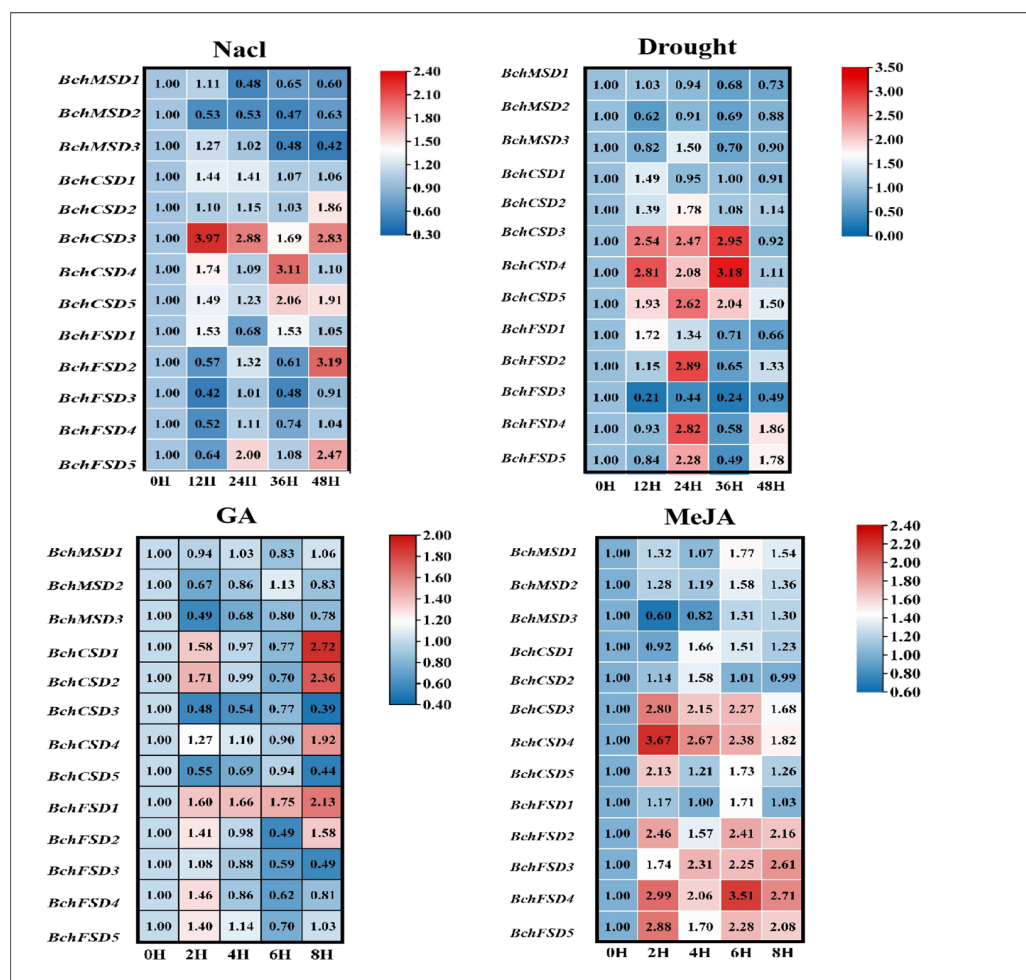


Figure 7. Expression of *BchSOD* genes under different abiotic stress and phytohormone conditions at different time points. The abiotic condition (salinity and drought) time points were 0 (CK), 12, 24, 36, and 48 h, and the phytohormone control (GA and MeJA) time points were 0 (CK), 2, 4, 6, and 8 h. The expression bands show comparative gene expression tendencies based on log₂ fold change values. Red represents high expression, and blue represents low expression.

3.9. Subcellular Localization of the *BchFSD2* Protein

Through preliminary analysis, we selected *BchFSD2*, which is abundantly expressed in leaves and significantly associated with abiotic stresses such as salt and drought, as well as hormones such as GA and MeJA, for subcellular localization studies. The cellular distribution of the *BchFSD2*-GFP fusion protein in the tobacco epidermis was further explored using the *Agrobacterium*-mediated tobacco transient expression system. The GFP

signature of the control expression vector was present in the nucleus, plasma membrane, and chloroplasts at the same time, and the BchFSD2-GFP fusion protein was expressed only in chloroplasts after transient expression in tobacco (Figure 8). This result suggested that the *BchFSD2* gene functions in chloroplasts.

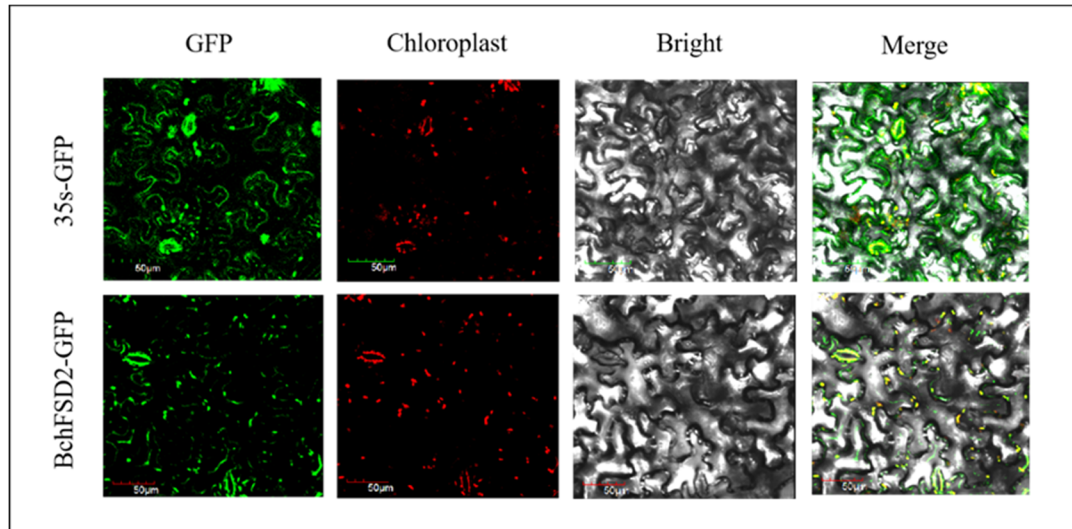


Figure 8. Subcellular localization of *BchFSD2* in tobacco epidermal cells. BchFSD2-GFP and 35s-GFP represent confocal images of the control empty vector and transient *BchFSD2* expression, respectively. GFP is the fluorescence field, Chloroplast is the chloroplast field, Bright is the bright field, and Merge is the superimposed field. The scale bar represents 50 μm .

3.10. Overexpression of the *BchFSD2* Gene Improves Salt Stress Tolerance in *Arabidopsis thaliana*

To further investigate the function of the *BchFSD2* gene under salt stress, we constructed a *BchFSD2* overexpression vector to transform *Arabidopsis thaliana* and investigated the gene function through changes in the phenotypes and physiological indices of the transgenic plants under salt stress (Figure 9). We subjected the transgenic plants (L1) and the WT plants to salt stress and established a control group for both L1 and WT, and significant phenotypic differences were observed between the plants after 9 days of salt stress treatment (Figure 9A). After PCR verification, it was determined that the target gene was successfully transferred into *Arabidopsis thaliana* (Figure 9B). Compared with those of the control plants, both the WT and L1 salt-stressed plants presented a yellow leaf color and plant dwarfing phenotype, but L1 presented fewer symptoms and was less inhibited than WT.

Furthermore, when plants are subjected to abiotic stresses such as salinity, massive quantities of ROS can accumulate in the plant body and threaten their growth, while the plant itself will maintain its own order through the production of antioxidants; thus, ROS and antioxidants are important indicators of the degree of injury to plants. Therefore, we measured CAT, POD, and SOD activities as well as superoxide anion and MDA contents (Figure 9C–G). During salt stress, the superoxide anion and MDA contents in L1 were significantly lower than those in WT, while in contrast, the antioxidant activity of CAT, POD, and SOD in L1 was markedly greater than that in WT. In conclusion, the differences in phenotypic and physiological indices suggest that the increase in salt tolerance in *BchFSD2* overexpressing plants may be mainly realized through the reduction of oxidative damage.

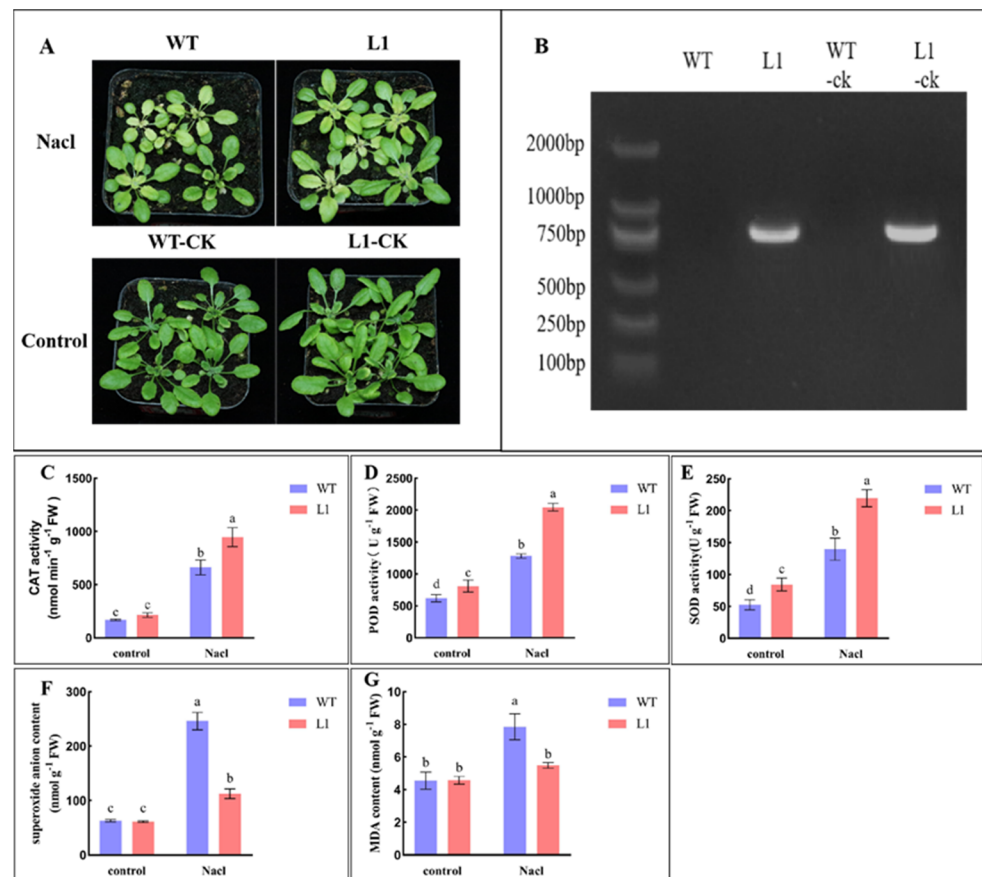


Figure 9. Overexpression of *BchFSD2* in *Arabidopsis thaliana*. (A) Plant growth phenotypes under salt stress. WT: wild type subjected to salt stress, L1: transgenic phenotype subjected to salt stress, WT-CK: wild type subjected to normal watering, L1-CK: normal watering transgenic type. (B) PCR validation plot of the overexpressed *BchFSD2* gene in transgenic plants. (C) CAT activity. (D) POD activity. (E) SOD activity. (F) Superoxide anion content. (G) MDA content. The data are presented as the standard errors of the means of three independent experiments ($n = 3$). Different letters indicate significant differences between treatments at $p < 0.005$.

4. Discussion

Pakchoi is an important crop that is widely grown and consumed in Asia because it is highly nutritious and can be consumed in a variety of ways [23]. Problems such as drought, high temperature, and salt stress can cause ROS accumulation in plants, which seriously affects the growth and development of pakchoi. In plant cells, SOD is a key enzyme in the first line of defense against ROS and is vital to plant physiological and biochemical processes because it plays a central role in protecting against the toxic effects of ROS generated by various environmental stresses [24]. Previous studies have all shown that SOD gene overexpression enhances resistance to abiotic stresses in plants such as *Arabidopsis* [25] and tobacco [26]. Current research on the SOD gene family in pakchoi is limited, and a complete exploration of SOD gene family characteristics and functions in pakchoi would be beneficial for enhancing the understanding of the SOD gene family in plants. Moreover, identifying and screening the best candidate genes associated with the response to abiotic stresses, such as salt stress in pakchoi, and performing in-depth analysis will be beneficial for subsequent investigations into how pakchoi responds to abiotic stresses.

In this study, we identified 13 SOD genes from the pakchoi genome, including three *Mn-SOD* genes, five *Cu/Zn-SOD* genes, and five *Fe-SOD* genes (Table 1), which were categorized into three groups according to their structural domains, namely MSD, CSD,

and FSD (Figure 1). Consistent with previous findings, the number of *SOD* family gene members in angiosperms has not expanded substantially during evolution and shows a highly conserved state; for example, eight *SOD* genes in *Arabidopsis* [27], thirteen *SOD* genes in maize [28], and nine *SOD* genes in tomato [11]. There may be some differences in the number of *SOD* genes in different plants due to the timing of gene duplications, including tandem and segmental duplications, as well as the effects of species evolution. The discovery of *SOD* gene doubling in a variety of plants by other researchers [10,29], in conjunction with our analyses, suggests that gene duplication may play a vital role in the evolution of *SOD* genes.

The three subfamilies of the *BchSOD* family also exhibited a high degree of conservation in terms of gene structure. By analyzing the number and distribution of exons and introns in the *BchSOD* genes, several differences in the number of exons and introns were found, but the differences within the same subfamily were small. Previous studies have shown that changes in exons and introns are the driving force of gene evolution and also directly lead to structural differences [30]. Further analysis also revealed that the intron-exon distribution patterns were similar within the same subfamily of the *BchSOD* family (Figure 2C). All these findings indicate that *BchSOD* was conserved during the evolutionary process. In addition, the analysis of the conserved structural domains showed that certain motifs existed only in certain subfamilies; for example, motif 9 was predicted only in the *Mn-SOD* subfamily, but some of the same motifs (motifs 1, 3, and 4) were also found in the *Fe-SOD* and *Mn-SOD* subfamilies (Figure 2B). These results suggest that *BchCSD* and the *BchFSD/BchMSD* may have different origins. In addition, motif analysis revealed that motifs 6, 7, and 9 were more conserved, and further analysis showed that members of the *Fe-SOD* and *Mn-SOD* subfamilies were more conserved (Figure 2D).

From the perspective of species evolution, gene duplication occurs in different ways throughout the evolutionary process and is an important pathway that drives the evolution of species [31]. The 13 *BchSOD* genes were analyzed at chromosomal locations, and all 11 genes had segmental duplication pairs except *BchMSD1* and *BchCSD5* (Figure 4). Additionally, by studying the collinearity of Pakchoi with closely related species (*A. thaliana* and *B. oleracea*), many *BchSOD* gene families were shown to have homologous gene pairs with *BolSOD* and *AtSOD* (Figure 5). These findings suggest that both segmental duplications and genome-wide duplications play important roles in the developmental evolution of the *BchSOD* family.

BchSODs are functionally diverse, and proteins play crucial roles in determining molecular function, both in terms of structure and properties [31]. Physical characterization of the *BchSOD* proteins revealed significant differences in protein sequence length, molecular weight, instability index, and isoelectric point among the 13 *BchSOD* proteins (Table 1). We also predicted and analyzed the 2D and 3D structures of the *BchSOD* proteins to gain a deeper understanding of the *BchSOD* proteins. According to our protein structure prediction (Figure S1 and Table S5), beta turns accounted for a greater percentage of the structure in the *Cu/ZnSOD* models than in the other two subfamilies, and their corresponding ligands were present in the structural models of the different subfamily proteins, with the exception of *BchFSD1*, *BchFSD4*, and *BchFSD5*. These predictions are consistent with previous 3D modeling of *SODs* in rapeseed [10], rice [32], and water lily [33].

To better understand the regulation of *SOD* gene expression in Pakchoi, we analyzed the cis-acting elements in the promoter. A large number of light-responsive, defense and stress, and hormone-responsive elements were found in the promoter region of the *BchSOD* gene through the prediction of 13 *BchSOD* gene promoter regions (Figure 3 and Table S4). The presence of drought-responsive elements (MBSs), anaerobic-responsive elements (AREs), low temperature-responsive elements (LTRs), and stress-responsive elements (TC-rich repeats) among the defense and stress-responsive related elements is in agreement with the fact that plant *SOD* genes play vital roles in plant defense and stress response [24]. A large number of researchers have shown that in plants such as *Arabidopsis thaliana* [34], rice [35], and tobacco [36], *SOD* genes contribute to plant resistance to abiotic

stresses. In addition, the promoter regions of the *BchSOD* genes were found to contain a series of cis-acting elements associated with phytohormone responses, such as abscisic-acid responsiveness elements (ABREs), MeJA- responsiveness elements (TGACG motif and CGTCA motif) and auxin-responsiveness elements (TGA elements). Previous researchers have also determined that *SOD* in plants is regulated by hormones such as ABA and MeJA by studying different plants [37–40]. It has also been found that gene expression in *SOD* transgenic tobacco plants is regulated by light [41], a phenomenon that is also in agreement with the abundance of light-related cis-acting elements we found in the *BchSOD* promoters. In conclusion, by analyzing cis-action elements, *BchSODs* were shown to be involved in the regulation of gene expression at different developmental stages in Pakchoi and to play an important role in the process of stress tolerance. These findings facilitate our understanding of *BchSODs* under different environmental conditions.

Plant *SOD* gene expression levels significantly change in different tissues and under different environmental conditions [10,11,34,42]. Therefore, we utilized qPCR to assess the tissue-specific expression levels of the *BchSOD* genes in four different regions (roots, petioles, cotyledons, and true leaves) (Figure 6 and Table S6). Compared with those of the other subfamilies, the FSD subfamily genes exhibited greater expression at all four sites, especially at the true leaf site. This result is comparable to the previous expression of tobacco *SOD* genes in different tissues [7]. In conclusion, the spatiotemporal expression of *BchSOD* family genes suggested that these genes are involved in different physiological activities.

Similarly, significant differences in *BchSOD* gene expression were detected under different hormones (GA and MeJA) and abiotic stress conditions (salt stress and drought stress) (Figure 7 and Table S7). Under salt stress and drought conditions, almost all the *BchSOD* genes, except for the *BchMSD2* gene, were upregulated within 48 h after treatment, especially *BchCSD3*, *BchCSD4*, and *BchFSD2*. These results are in accordance with the results of previous studies. *SOD* genes are upregulated in both tomato and wheat plants under drought and salt stress conditions [11,43]. Different *SOD* genes were also found in maize at different times in response to salt and drought stress, suggesting that *ZmSODs* may have different regulatory mechanisms in response to salt and drought stress [28]. Taken together, the results of previous studies and our findings demonstrate that *SOD* genes exert conserved effects on plant abiotic stress and that different *SOD* genes have different mechanisms involved in the response to stress. Additionally, in the hormonal (GA and MeJA) environments, all the genes were upregulated from 0 h to 8 h, except for *BchMSD3* and *BchCSD3*, which were downregulated GA treatment. Moreover, we found that the expression of several genes (*BchCSD1*, *BchCSD2*, *BchCSD4*, and *BchFSD1*) significantly increased in response to GA treatment, while the expression of the *BchCSD3*, *BchCSD4*, *BchFSD2*, *BchFSD3*, *BchFSD4*, and *BchFSD5* genes significantly increased in response to externally applied MeJA. Several studies have already shown that phytohormones can resist stress by activating signaling transcriptional pathways [44]. Similarly, in tea trees, several CSD and FSD genes were found to respond to exogenous GA and MeJA, and the majority of *SOD* genes were upregulated in rapeseed in response to GA, ABA, and other stress treatments [10,45]. According to previous studies and analyses, most of the *BchSOD* gene expression is regulated by external hormones and abiotic stresses, and the stress resistance of Pakchoi plants is enhanced by increased gene expression.

Based on previous studies on the *BchSOD* gene family, we found that *BchFSD2* was not only abundantly expressed on leaves but also sensitive to salt stresses; therefore, we hypothesized that the *BchFSD2* gene may play an essential role in the response to abiotic stress in pakchoi. Phenotypic and physiological parameters of control and *BchFSD2* gene overexpressing Arabidopsis plants subjected to simulated salt stress indicated that the *BchFSD2* gene indeed plays a role in plant resistance to salt stress and that it likely enhances plant resistance to salt stress and that it likely enhances plant tolerance to salt stress by increasing the ROS removal activity of the plant (Figures 9 and 10). The overexpression of *SOD* genes in plants such as tobacco [46–48], Arabidopsis thaliana, and tall fescue has been previously performed, and the transgenic plants were found to exhibit similar

characteristics increase plant oxidative stress protection by enhancing the reactive oxygen species scavenging system, which is consistent with our findings.

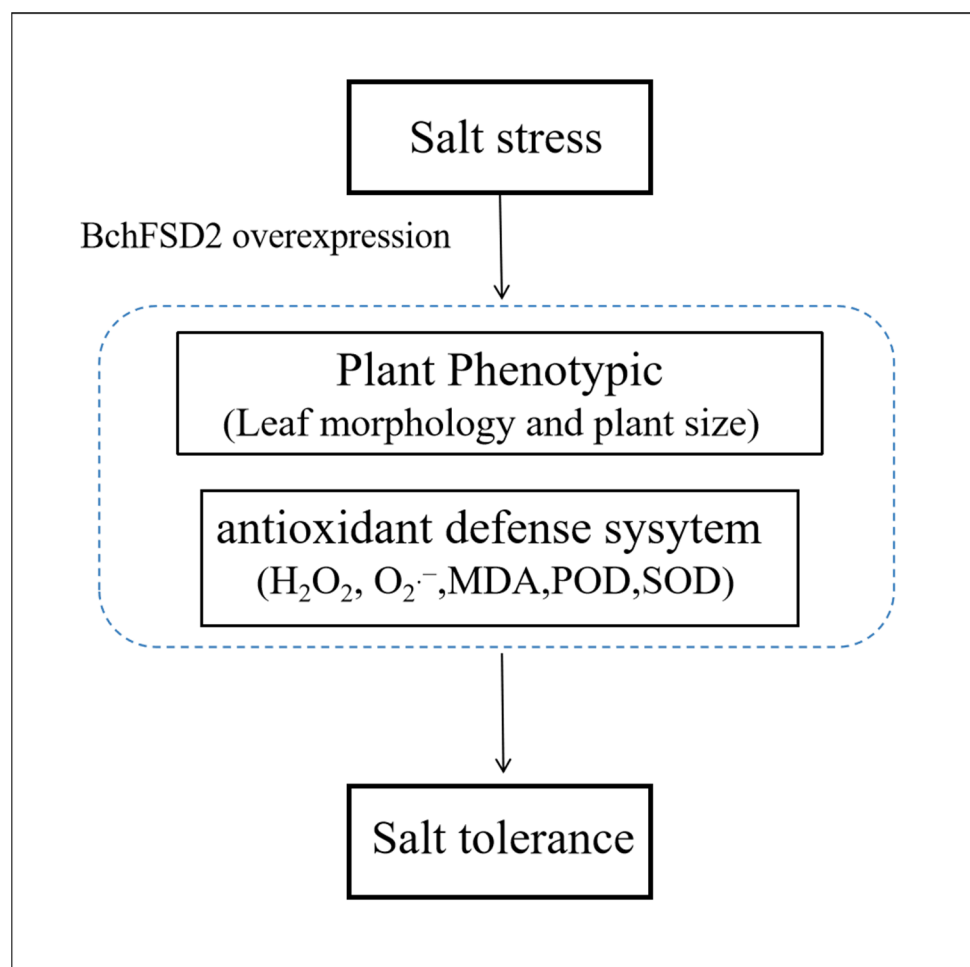


Figure 10. *BchFSD2* gene overexpression regulating the modeling diagram of pakchoi tolerance to salt stress. The blue dashed box represents the changes in plants under salt stress.

5. Conclusions

In this study, a comprehensive gene family-wide analysis of the *SOD* gene family of pakchoi was performed, and 13 *BchSOD* genes were identified. The physicochemical properties, phylogeny, gene structure, conserved structural domains, cis-elements, chromosomal localization and collinearity relationships, tissue-specific expression, and expression profiles of the *BchSOD* genes were investigated, and it was concluded that the *BchSOD* genes play essential roles in the response to hormonal and abiotic stresses. Moreover, the *BchFSD2* gene, which is sensitive to salt, will be studied in depth as a key candidate gene for plant resistance to abiotic stresses. The overexpression of the *BchFSD2* gene in *Arabidopsis thaliana* increased the plant antioxidant enzyme activity, thereby increasing plant tolerance to salt stress. These findings provide new possibilities for *BchFSD2* to regulate salt tolerance in pakchoi and provide a new theoretical basis for a more comprehensive understanding of *SOD* gene function in pakchoi.

Supplementary Materials: The following supporting information can be downloaded at <https://www.mdpi.com/article/10.3390/agronomy14020384/s1>, Table S1: A list of primers used for gene expression analysis by qRT-PCR. Table S2: A list of primers used for gene-specific amplification. Table S3: Detailed information on 10 identified motifs in *BchSOD* proteins. Table S4: Information on hormone- and stress-related cis-elements detected in the promoter regions of *BchSOD* genes. Table S5:

Detailed information on the 2D and 3D structures of *BchSOD* proteins. Table S6: The expression profiles of *BchSOD* genes in different tissues. Table S7: The expression profiles of *BchSOD* genes under abiotic stresses and exogenous phytohormones. Figure S1. Predicted 3D structures of the *BchSOD* proteins. The dots in the figure represent ligands, the blue bars represent alpha helices, and the green bars represent beta turns. Figure S2. Phylogenetic tree of *SOD* proteins from *A. thaliana*, *B. oleracea*, *B. napus*, and *B. chinensis*. (the maximal method). Figure S3. Phylogenetic tree of *SOD* proteins from *A. thaliana*, *B. oleracea*, *B. napus*, and *B. chinensis*. (the minimal method).

Author Contributions: Conceptualization, F.Z., Y.Z., M.H. (Maomao Hou) and S.L.; methodology, Y.Z.; software, S.R. and Y.Z.; validation, Y.X. and Y.Z.; formal analysis, Y.Z.; investigation, M.H. (Mingxuan Han); resources, S.L.; data curation, S.R.; writing—original draft preparation, Y.Z.; writing—review and editing, S.L., Y.Z. and F.Z.; visualization, Y.Z.; supervision, S.R.; funding acquisition, F.Z. All authors have read and agreed to the published version of the manuscript.

Funding: This work was supported by the National Key Programs for Bok Choy Breeding of China (111821301354052283), the Fujian Modern Agricultural Vegetable Industry System Construction Project (2019-897), the Seed Industry Innovation and Industrialization Project in Fujian Province (zyxcny2021009), and the Fuzhou Science and Technology Project (2022-P-001; 2022-P-018).

Data Availability Statement: Data are contained within the article and Supplementary Materials.

Conflicts of Interest: The authors declare no conflicts of interest.

References

- Zhu, J.K. Abiotic Stress Signaling and Responses in Plants. *Cell* **2016**, *167*, 313–324. [[CrossRef](#)] [[PubMed](#)]
- Del Río, L.A. ROS and RNS in plant physiology: An overview. *J. Exp. Bot.* **2015**, *66*, 2827–2837. [[CrossRef](#)] [[PubMed](#)]
- Hasanuzzaman, M.; Bhuyan, M.B.; Zulfiqar, F.; Raza, A.; Mohsin, S.M.; Mahmud, J.A.; Fujita, M.; Fotopoulos, V. Reactive Oxygen Species and Antioxidant Defense in Plants under Abiotic Stress: Revisiting the Crucial Role of a Universal Defense Regulator. *Antioxidants* **2020**, *9*, 681. [[CrossRef](#)] [[PubMed](#)]
- Gill, S.S.; Tuteja, N. Reactive oxygen species and antioxidant machinery in abiotic stress tolerance in crop plants. *Plant Physiol. Biochem.* **2010**, *48*, 909–930. [[CrossRef](#)]
- Rajput, V.D.; Harish; Singh, R.K.; Verma, K.K.; Sharma, L.; Quiroz-Figueroa, F.R.; Meena, M.; Gour, V.S.; Minkina, T.; Sushkova, S.; et al. Recent Developments in Enzymatic Antioxidant Defence Mechanism in Plants with Special Reference to Abiotic Stress. *Biology* **2021**, *10*, 267. [[CrossRef](#)]
- Pilon, M.; Ravet, K.; Tapken, W. The biogenesis and physiological function of chloroplast superoxide dismutases. *Biochim. Biophys. Acta BBA Bioenerg.* **2011**, *1807*, 989–998. [[CrossRef](#)]
- Huo, C.; He, L.; Yu, T.; Ji, X.; Li, R.; Zhu, S.; Zhang, F.; Xie, H.; Liu, W. The Superoxide Dismutase Gene Family in *Nicotiana tabacum*: Genome-Wide Identification, Characterization, Expression Profiling and Functional Analysis in Response to Heavy Metal Stress. *Front. Plant Sci.* **2022**, *13*, 904105. [[CrossRef](#)]
- Shiraya, T.; Mori, T.; Maruyama, T.; Sasaki, M.; Takamatsu, T.; Oikawa, K.; Itoh, K.; Kaneko, K.; Ichikawa, H.; Mitsui, T. Golgi/plastid-type manganese superoxide dismutase involved in heat-stress tolerance during grain filling of rice. *Plant Biotechnol. J.* **2015**, *13*, 1251–1263. [[CrossRef](#)]
- Mosa, K.A.; El-Naggar, M.; Ramamoorthy, K.; Alawadhi, H.; Elnaggar, A.; Wartanian, S.; Ibrahim, E.; Hani, H. Copper Nanoparticles Induced Genotoxicity, Oxidative Stress, and Changes in Superoxide Dismutase (*SOD*) Gene Expression in Cucumber (*Cucumis sativus*) Plants. *Front. Plant Sci.* **2018**, *9*, 872. [[CrossRef](#)]
- Su, W.; Raza, A.; Gao, A.; Jia, Z.; Zhang, Y.; Hussain, M.A.; Mehmood, S.S.; Cheng, Y.; Lv, Y.; Zou, X. Genome-Wide Analysis and Expression Profile of Superoxide Dismutase (*SOD*) Gene Family in Rapeseed (*Brassica napus* L.) under Different Hormones and Abiotic Stress Conditions. *Antioxidants* **2021**, *10*, 1182. [[CrossRef](#)]
- Feng, K.; Yu, J.; Cheng, Y.; Ruan, M.; Wang, R.; Ye, Q.; Zhou, G.; Li, Z.; Yao, Z.; Yang, Y.; et al. The *SOD* Gene Family in Tomato: Identification, Phylogenetic Relationships, and Expression Patterns. *Front. Plant Sci.* **2016**, *7*, 1279. [[CrossRef](#)]
- Han, X.-M.; Chen, Q.X.; Yang, Q.; Zeng, Q.Y.; Lan, T.; Liu, Y.J. Genome-wide analysis of superoxide dismutase genes in *Larix kaempferi*. *Gene* **2019**, *686*, 29–36. [[CrossRef](#)] [[PubMed](#)]
- Han, L.; Hua, W.P.; Cao, X.Y.; Yan, J.A.; Chen, C.; Wang, Z.Z. Genome-wide identification and expression analysis of the superoxide dismutase (*SOD*) gene family in *Salvia miltiorrhiza*. *Gene* **2020**, *742*, 144603. [[CrossRef](#)] [[PubMed](#)]
- Hu, X.; Hao, C.; Cheng, Z.-M.; Zhong, Y. Genome-Wide Identification, Characterization, and Expression Analysis of the Grapevine Superoxide Dismutase (*SOD*) Family. *Int. J. Genom.* **2019**, *2019*, e7350414. [[CrossRef](#)]
- Yu, W.; Kong, G.; Chao, J.; Yin, T.; Tian, H.; Ya, H.; He, L.; Zhang, H. Genome-wide identification of the rubber tree superoxide dismutase (*SOD*) gene family and analysis of its expression under abiotic stress. *PeerJ* **2022**, *10*, e14251. [[CrossRef](#)] [[PubMed](#)]
- Anwar, A.; Zhang, S.; Wang, L.; Wang, F.; He, L.; Gao, J. Genome-Wide Identification and Characterization of Chinese Cabbage *S1fa* Transcription Factors and Their Roles in Response to Salt Stress. *Antioxidants* **2022**, *11*, 1782. [[CrossRef](#)]

17. Chen, C.; Wu, Y.; Xia, R. A painless way to customize Circos plot: From data preparation to visualization using TBtools. *iMeta* **2022**, *1*, e35. [[CrossRef](#)]
18. Kumar, S.; Stecher, G.; Li, M.; Knyaz, C.; Tamura, K. MEGA X: Molecular Evolutionary Genetics Analysis across Computing Platforms. *Mol. Biol. Evol.* **2018**, *35*, 1547. [[CrossRef](#)] [[PubMed](#)]
19. Subramanian, B.; Gao, S.; Lercher, M.J.; Hu, S.; Chen, W.-H. Evolvview v3: A webserver for visualization, annotation, and management of phylogenetic trees. *Nucleic Acids Res.* **2019**, *47*, W270–W275. [[CrossRef](#)]
20. Waterhouse, A.; Bertoni, M.; Bienert, S.; Studer, G.; Tauriello, G.; Gumienny, R.; Heer, F.T.; de Beer, T.A.P.; Rempfer, C.; Bordoli, L.; et al. SWISS-MODEL: Homology modelling of protein structures and complexes. *Nucleic Acids Res.* **2018**, *46*, W296–W303. [[CrossRef](#)]
21. Livak, K.J.; Schmittgen, T.D. Analysis of relative gene expression data using real-time quantitative PCR and the $2^{-\Delta\Delta C(T)}$ Method. *Methods* **2001**, *25*, 402–408. [[CrossRef](#)] [[PubMed](#)]
22. Clough, S.J.; Bent, A.F. Floral dip: A simplified method for *Agrobacterium*-mediated transformation of *Arabidopsis thaliana*. *Plant J.* **1998**, *16*, 735–743. [[CrossRef](#)]
23. Lyu, X.; Ng, K.R.; Mark, R.; Lee, J.L.; Chen, W.N. Comparative metabolic profiling of engineered *Saccharomyces cerevisiae* with enhanced flavonoids production. *J. Funct. Foods* **2018**, *44*, 274–282. [[CrossRef](#)]
24. Wang, W.; Xia, M.X.; Chen, J.; Yuan, R.; Deng, F.N.; Shen, F.F. Gene expression characteristics and regulation mechanisms of superoxide dismutase and its physiological roles in plants under stress. *Biochemistry* **2016**, *81*, 465–480. [[CrossRef](#)]
25. Shafi, A.; Chauhan, R.; Gill, T.; Swarnkar, M.K.; Sreenivasulu, Y.; Kumar, S.; Kumar, N.; Shankar, R.; Singh Ahuja, P.; Singh, A.K. Expression of *SOD* and *APX* genes positively regulates secondary cell wall biosynthesis and promotes plant growth and yield in *Arabidopsis* under salt stress. *J. Plant Mol. Biol.* **2015**, *87*, 615–631. [[CrossRef](#)]
26. Pan, C.; Lu, H.; Yu, J.; Liu, J.; Liu, Y.; Yan, C. Identification of Cadmium-responsive *Kandelia obovata* *SOD* family genes and response to Cd toxicity. *Environ. Exp. Bot.* **2019**, *162*, 230–238. [[CrossRef](#)]
27. Gharari, Z.; Nejad, R.K.; Band, R.S.; Najafi, F.; Nabiyuni, M.; Irian, S. The role of *Mn-SOD* and *Fe-SOD* genes in the response to low temperature in chs mutants of *Arabidopsis*. *Turk. J. Bot.* **2014**, *38*, 80–88. [[CrossRef](#)]
28. Liu, J.; Xu, L.; Shang, J.; Hu, X.; Yu, H.; Wu, H.; Lv, W.; Zhao, Y. Genome-wide analysis of the maize superoxide dismutase (*SOD*) gene family reveals important roles in drought and salt responses. *Genet. Mol. Biol.* **2021**, *44*, e20210035. [[CrossRef](#)]
29. Verma, D.; Lakhanpal, N.; Singh, K. Genome-wide identification and characterization of abiotic-stress responsive *SOD* (superoxide dismutase) gene family in *Brassica juncea* and *B. rapa*. *BMC Genom.* **2019**, *20*, 227. [[CrossRef](#)]
30. Xu, G.; Guo, C.; Shan, H.; Kong, H. Divergence of duplicate genes in exon–intron structure. *Proc. Natl. Acad. Sci. USA* **2012**, *109*, 1187–1192. [[CrossRef](#)]
31. Mohanta, T.K.; Khan, A.; Hashem, A.; Abd_Allah, E.F.; Al-Harrasi, A. The molecular mass and isoelectric point of plant proteomes. *BMC Genom.* **2019**, *20*, 631. [[CrossRef](#)]
32. Song, J.; Zeng, L.; Chen, R.; Wang, Y.; Zhou, Y. In silico identification and expression analysis of superoxide dismutase (*SOD*) gene family in *Medicago truncatula*. *3 Biotech* **2018**, *8*, 348. [[CrossRef](#)] [[PubMed](#)]
33. Khan, W.U.; Khan, L.U.; Chen, D.; Chen, F. Comparative Analyses of Superoxide Dismutase (*SOD*) Gene Family and Expression Profiling under Multiple Abiotic Stresses in Water Lilies. *Horticulturae* **2023**, *9*, 781. [[CrossRef](#)]
34. Hunt, L.; Otterhag, L.; Lee, J.C.; Lasheen, T.; Hunt, J.; Seki, M.; Shinozaki, K.; Sommarin, M.; Gilmour, D.J.; Pical, C.; et al. Gene-specific expression and calcium activation of *Arabidopsis thaliana* phospholipase C isoforms. *New Phytol.* **2004**, *162*, 643–654. [[CrossRef](#)] [[PubMed](#)]
35. Wang, F.-Z.; Wang, Q.-B.; Kwon, S.-Y.; Kwak, S.-S.; Su, W.-A. Enhanced drought tolerance of transgenic rice plants expressing a pea manganese superoxide dismutase. *J. Plant Physiol.* **2005**, *162*, 465–472. [[CrossRef](#)] [[PubMed](#)]
36. Faize, M.; Burgos, L.; Faize, L.; Petri, C.; Barba-Espin, G.; Diaz-Vivancos, P.; Clemente-Moreno, M.J.; Alburquerque, N.; Hernandez, J.A. Modulation of tobacco bacterial disease resistance using cytosolic ascorbate peroxidase and Cu, Zn-superoxide dismutase. *Plant Pathol.* **2012**, *61*, 858–866. [[CrossRef](#)]
37. Agarwal, S.; Sairam, R.K.; Srivastava, G.C.; Tyagi, A.; Meena, R.C. Role of ABA, salicylic acid, calcium and hydrogen peroxide on antioxidant enzymes induction in wheat seedlings. *Plant Sci.* **2005**, *169*, 559–570. [[CrossRef](#)]
38. Castillo, S.; Martínez Romero, D.; Guillén, F.; Sayyari, M.; Zapata, P.J. Methyl jasmonate treatment reduces chilling injury and improves antioxidant activity. In *Options Méditerranéennes Séries A: Mediterranean Seminars*; Universidad Miguel Hernández: Elche, Spain, 2012.
39. Jiang, L.; Jin, P.; Wang, L.; Yu, X.; Wang, H.; Zheng, Y. Methyl jasmonate primes defense responses against *Botrytis cinerea* and reduces disease development in harvested table grapes. *Sci. Hortic.* **2015**, *192*, 218–223. [[CrossRef](#)]
40. Lu, S.; Su, W.; Li, H.; Guo, Z. Abscisic acid improves drought tolerance of triploid bermudagrass and involves H_2O_2 - and NO-induced antioxidant enzyme activities. *Plant Physiol. Biochem.* **2009**, *47*, 132–138. [[CrossRef](#)]
41. Tsang, E.W.T. Differential Regulation of Superoxide Dismutases in Plants Exposed to Environmental Stress. *Plant Cell* **1991**, *3*, 783–792.
42. Zhou, Y.; Hu, L.; Wu, H.; Jiang, L.; Liu, S. Genome-Wide Identification and Transcriptional Expression Analysis of Cucumber Superoxide Dismutase (*SOD*) Family in Response to Various Abiotic Stresses. *Int. J. Genom.* **2017**, *2017*, e7243973. [[CrossRef](#)]
43. Jiang, W.; Yang, L.; He, Y.; Zhang, H.; Li, W.; Chen, H.; Ma, D.; Yin, J. Genome-wide identification and transcriptional expression analysis of superoxide dismutase (*SOD*) family in wheat (*Triticum aestivum*). *PeerJ* **2019**, *7*, e8062. [[CrossRef](#)] [[PubMed](#)]

44. Raja, V.; Majeed, U.; Kang, H.; Andrabi, K.I.; John, R. Abiotic stress: Interplay between ROS, hormones and MAPKs. *Environ. Exp. Bot.* **2017**, *137*, 142–157. [[CrossRef](#)]
45. Zhou, C.; Zhu, C.; Fu, H.; Li, X.; Chen, L.; Lin, Y.; Lai, Z.; Guo, Y. Genome-wide investigation of superoxide dismutase (SOD) gene family and their regulatory miRNAs reveal the involvement in abiotic stress and hormone response in tea plant (*Camellia sinensis*). *PLoS ONE* **2019**, *14*, e0223609. [[CrossRef](#)] [[PubMed](#)]
46. Gupta, A.S.; Webb, R.P.; Holaday, A.S.; Allen, R.D. Overexpression of Superoxide Dismutase Protects Plants from Oxidative Stress (Induction of Ascorbate Peroxidase in Superoxide Dismutase-Overexpressing Plants). *Plant Physiol.* **1993**, *103*, 1067–1073. [[CrossRef](#)]
47. Wang, Y.; Ying, Y.; Chen, J.; Wang, X. Transgenic Arabidopsis overexpressing *Mn-SOD* enhanced salt-tolerance. *Plant Sci.* **2004**, *167*, 671–677. [[CrossRef](#)]
48. Lee, S.H.; Ahsan, N.; Lee, K.W.; Kim, D.H.; Lee, D.G.; Kwak, S.S.; Kwon, S.Y.; Kim, T.H.; Lee, B.H. Simultaneous overexpression of both CuZn superoxide dismutase and ascorbate peroxidase in transgenic tall fescue plants confers increased tolerance to a wide range of abiotic stresses. *J. Plant Physiol.* **2007**, *164*, 1626–1638. [[CrossRef](#)]

Disclaimer/Publisher’s Note: The statements, opinions and data contained in all publications are solely those of the individual author(s) and contributor(s) and not of MDPI and/or the editor(s). MDPI and/or the editor(s) disclaim responsibility for any injury to people or property resulting from any ideas, methods, instructions or products referred to in the content.